

# LTSPICE IV Simulation of H<sup>+</sup> Ion FET

<sup>a</sup>NUR LIYANA MARDHIAH, <sup>a,b</sup>LEE YOOT KHUAN and <sup>a</sup>ROZIAH JARMIN

<sup>a</sup>Faculty of Electrical Engineering

<sup>b</sup>Computational Intelligence Detection RIG

Pharmaceutical & Lifesciences Communities of Research

Universiti Teknologi MARA, Shah Alam, Selangor DE, Malaysia

leeyootkuan@salam.uitm.edu.my

**Abstract:** - pH measurement has been reported in many applications as a key parameter, such as clinical analysis, food production, biotechnology processes, wastewater treatment, environmental and life sciences. Advances in FET technology introduces a chemical effect transistor, the Ion Selective Field Effect Transistor (ISFET), which can convert the activity of ions in electrolyte into electrical potential. It has the potential of an integrated detection system. It is cost effective if design of such a measurement system can be assessed and improved using a simulator such as LTSPICE, before the costly fabrication. However, the ISFET macromodel is not listed as a component in the LTSPICE IV component library. Our work here describes the development of an ISFET macromodel in LTSPICE IV. It started with derivation of the mathematical models, building of the netlist and explanation on the procedure to include as library component. From simulation result, the drain current is found to vary with pH, arises from the variation in the concentration of the H<sup>+</sup> ion. Low pH or acidic solution produces high value of I<sub>d</sub>, when concentration of H<sup>+</sup> ion concentration is high in the electrolyte solution.

**Key-Words:** - ISFET; LTSPICE IV; H<sup>+</sup> Ion; pH

## 1 Introduction

Variable pH has long been acknowledged as the most important parameter that indicates the physical properties of solution [1][2]. It is an abbreviation for *pondus hydrogenii*, meaning the weight of hydrogen, introduced by the Danish biochemist, S. P. L. Sørensen, in 1909 [3]. The original logarithmic definition created by Sorensen is as in (1) [4]:

$$pH = -\log[H^+] \quad (1)$$

where [H<sup>+</sup>] is the concentration of hydrogen ion in mol/L, which depends on the activity of the ion in the aqueous solution. Later, in 1924, pH has been revised to adapt definition and measurement in terms of electrochemical cells as in (2) [5]:

$$pH = [H^+]/[OH^-] \quad (2)$$

where [H<sup>+</sup>] and [OH<sup>-</sup>] are concentration of hydrogen and hydroxide ion. Its value ranges from pH0 to pH14 [6]. The solution is acidic if the [H<sup>+</sup>] is greater than [OH<sup>-</sup>] and the pH value will be less than pH7. Conversely, if the [OH<sup>-</sup>] is greater than the [H<sup>+</sup>], the solution is alkaline and the pH value will be more than pH7. If the ratio of [H<sup>+</sup>] to [OH<sup>-</sup>] is equal, the solution is neutral at pH7 [7].

pH measurement are known to be used successfully in clinical analysis, food production, biotechnology processes, wastewater treatment, environmental and life sciences [8][9]. It has been reported that pH measurement has been applied in many applications as a key parameter. From literature, pH value is an important parameter for therapeutic intervention in wound-care [10]. In addition, pH value is also an important parameter in the study of tissue metabolism, in neurophysiology and cancer diagnostics[1]. More so, most of the things we used in our daily life are tested by pH measurement such as tap water, cosmetics and medicines [5].

Subsequent to the primitive method of pH measurement by using chemical indicators, such as litmus paper [11], metal electrode such as glass electrode has successfully been devised [12]. Nevertheless, the glass electrode were found not applicable for many operations. This is because it is unstable at high temperature, brittle and difficult to miniaturize, therefore unsuitable for food, in-vivo and similar applications [12]

Advance in technology introduces a chemical effect transistor, the Ion Selective Field Effect Transistor (ISFET) [13]. Fundamentally, it is a sensor that converts the activity of a specific ion dissolved in a solution into an electrical potential, which can be measured by a measuring instruments[14]. From

principle operation of ISFET, the gate voltage of ISFET changes accordance to the H<sup>+</sup> ion concentration. The glass-less and small-sized sensor have been shown implementable with current detection method of H<sup>+</sup> ions concentration with potential for an integrated detection system [13][16][17]. It is cost effective if design of a measurement system can be assessed and improved using a simulator such as LTSPICE, before the costly fabrication. However, the ISFET macromodel is not listed as a component in the LTSPICE IV component library.

The purpose of our work here is to develop an ISFET macromodel by using LTSPICE IV software to allow simulation of the ISFET operation. The next section studies the characteristics and the relationship of the ISFET variables to derive the mathematical models. Section 3 describes how the models are integrated to construct the ISFET macromodel in LTSPICE IV. And finally, results from the simulation of the functions of ISFET macromodel with LTSPICE IV software are discussed.

## 2 Mathematical Model of ISFET

ISFET mathematic model can be represented by two mutually independent models, electrochemical model and electrical model. The electrochemical model describes the electrolyte insulator interface while the electrical model describes the structure of ISFET. The electrical model is acquired subsequent to the electrochemical model of ISFET, with derivation of each component as explained in this section.

The following presents the equivalent of electrical model of ISFET from node 1 to node 10 as displayed in Fig. 1. When the ISFET is at the static stage, the reference voltage can be expressed as (3) and (4) [15].

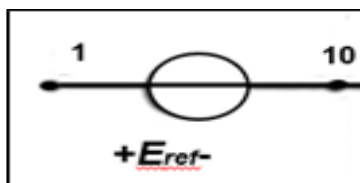


Fig. 1 Reference voltage, E<sub>ref</sub>

$$E_{ref} = [X] + \phi_{eo} + \phi_{lj} \quad (3)$$

$$[X] = (E_{abs} - \phi_m - E_{rel}) \quad (4)$$

where E<sub>ref</sub> is reference electrode, E<sub>abs</sub> is absolute potential of the reference electrode of the standard hydrogen,  $\phi_m$  is work function of the metal back contact or electronic electrode relative to the hydrogen electrode,  $\phi_{eo}$  is surface dipole potential and  $\phi_{lj}$  is liquid junction potential difference between the reference solution and electrolyte while E<sub>rel</sub> is the potential of the reference.

The following presents equivalent of electrical model of ISFET from node 10 to node 2 as shown in Fig. 2. The equivalent capacitor, C<sub>eq</sub>, represents the capacitance in series, C<sub>Gouy</sub> of diffuse layer and C<sub>Helm</sub> of Helmholtz layer as below [16]:

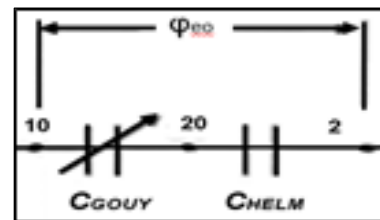


Fig. 2 Equivalent capacitor, C<sub>eq</sub>

$$C_{eq} = \left( \frac{C_{Gouy} C_{Helm}}{C_{Gouy} + C_{Helm}} \right) \quad (5)$$

Prior to the next node, the condition of charge neutrality in ISFET electrochemical model had to be taken into account by assuming that  $\sigma_s$  is very small relative to  $\sigma_o$  and  $\sigma_d$ , in fact constant in pH [16],

$$\sigma_o + \sigma_d = 0 \quad (6)$$

where  $\sigma_o$ ,  $\sigma_d$  and  $\sigma_s$  are charge densities at the electrolyte insulator interface and diffuse layer in the semiconductor. Hence,  $\sigma_o$  and  $\sigma_d$  are defined as follow based on H<sup>+</sup> specific site binding theory and electrical binding theory [16],

$$\sigma_d = \sqrt{8\epsilon_w kT} c_{bulk} \sinh\left(\frac{\phi_d}{2V_T}\right) \quad (7)$$

$$\sigma_d = q[A] + [B] \quad (8)$$

$$[A] = \left[ \frac{e^{\left(-2\frac{\phi_{eo}}{V_T}\right) - e^{(\log K_a K_b + 4.6(H_b))}}}{e^{\left(-2\frac{\phi_{eo}}{V_T}\right) + \left[e^{(\log K_a + 2.3(H_b))}\right] e^{\left(-\frac{\phi_{eo}}{V_T}\right)}} + e^{(\log K_a K_b + 4.6(H_b))}} \right] N_{sil} \quad (9)$$

$$[B] = \left[ N_{nit} \frac{e \left( -\frac{\varphi_{eo}}{V_T} \right)}{e \left( -\frac{\varphi_{eo}}{V_T} \right) + \frac{K_n}{K_a} e(\log K_a + 2.3(H_b))} \right] \quad (10)$$

where  $\epsilon_w$  and  $c_{bulk}$  is the permittivity and ion concentration of electrolyte,  $N_{sil}$  and  $N_{nit}$ ;  $\varphi_{gd}$  is the potential across the diffusion layer;  $V_T$  is the thermal voltage;  $K_a$ ,  $K_b$ ,  $K_n$  are the binding sites dissociation constants;  $H_b$  is the proton concentration of the bulk electrolyte;  $\varphi_{eo}$  is potential of the electrolyte insulator interface.  $k$  is boltzman constant and  $T$  is the temperature.

Therefore, by substituting (5) into equation (8), the charge densities at the electrolyte insulator interface becomes [15],

$$\sigma_o = [N_{sil} f_a(\varphi_{eo}, pH) + N_{nit}(\varphi_{eo}, pH)] \quad (11)$$

which gives rise to the potential of the electrolyte insulator interface,

$$\varphi_{eo} = \frac{q}{C_{eq}} [N_{sil} f_a(\varphi_{eo}, pH) + N_{nit}(\varphi_{eo}, pH)] \quad (12)$$

Then drain source current,  $I_{ds}$  and gate-source voltage,  $V_{gs}$  depend on potential of the electrolyte insulator interface,  $\varphi_{eo}$  and  $pH$ . The  $pH$ -independent source is designated as a chemical input signal, modeled by an independent voltage source, connected to a dummy resistor. The macromodel uses the voltage to simulate the  $pH$  value.

Hence, the physical ISFET from node 2 to node 4, in Fig. 3 is obtained as follows based on the MOSFET theory:

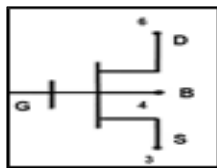


Fig. 3 Physical ISFET

$$I_{DS} \approx k_p (\Delta) V_{DS} \quad (13)$$

$$k_p = \mu_n C_{eq} W / L \quad (14)$$

$$\Delta = (V_{GS} - V_{TH}^*) \quad (15)$$

$$V_{TH}^* = V_{TH} + E_{PH} \quad (16)$$

$$E_{PH} = \varphi_{eo} \quad (17)$$

where  $k_p$  is device transductance factor,  $V_{TH}$  is the threshold voltage,  $V_{ds}$  is the drain source voltage,  $\mu_n$  is electron mobility and  $E_{PH}$  is equal to  $\varphi_{eo}$ .

### 3 Methodology

The independent mathematical models as shown in Fig. 1, 2 and 3 in Section 2 were assembled into the workflow as in Fig. 4.

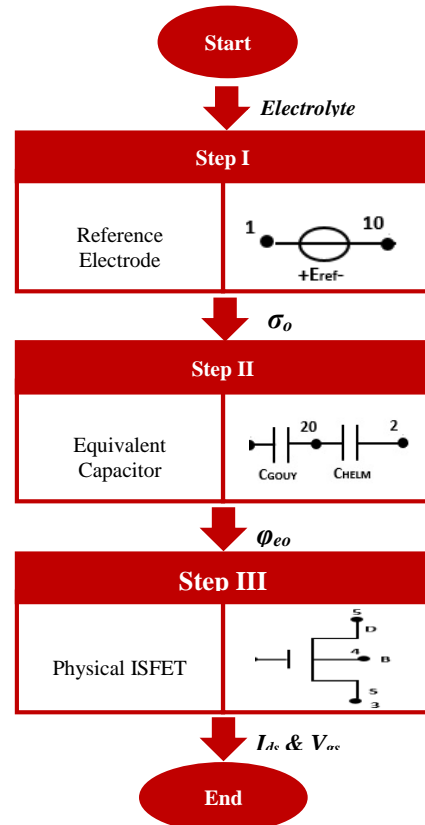


Fig. 4 Simulation model of ISFET assembled from mathematical model.

When the electrochemical is in static behavior,  $E_{ref}$  can be derived as equation (3). When the reference electrode is exposed, it produces the charge densities,  $\sigma_o$ . Based on  $H^+$  specific binding theory and electrical double layer theory, the produced charge densities can be defined as equation (8) in Section 2.

The produced charge densities generates a potential of the electrolyte at the electrolyte insulator interface,  $\varphi_{eo}$  which give the relations as equation (12) in Section 2.

Capacitance in series,  $C_{GOUY}$  of diffuse layer and  $C_{HELM}$  of Helmholtz layer as in Fig. 4 can be substituted by the equivalent capacitor  $C_{eq}$  in equation (5) of Section 2.

Lastly at the electrical stage, the source-drain current ( $I_{ds}$ ) and the source-gate voltage ( $V_{gs}$ ),

output of physical ISFET in Fig. 4, can be obtained from equation (13) of Section 2. From the derivation of equation (13), the potential of the electrolyte of the electrolyte insulator interface,  $\phi_{eo}$  was obtained as equation (17) in Section 2.

Next, the mathematical equations from assembly of the simulation ISFET model was integrated and converted into netlists as shown in Step 1 of Fig.5. Then the netlists are then implemented in LTSPICE IV software, as shown in Step 2-4 of Fig. 5.

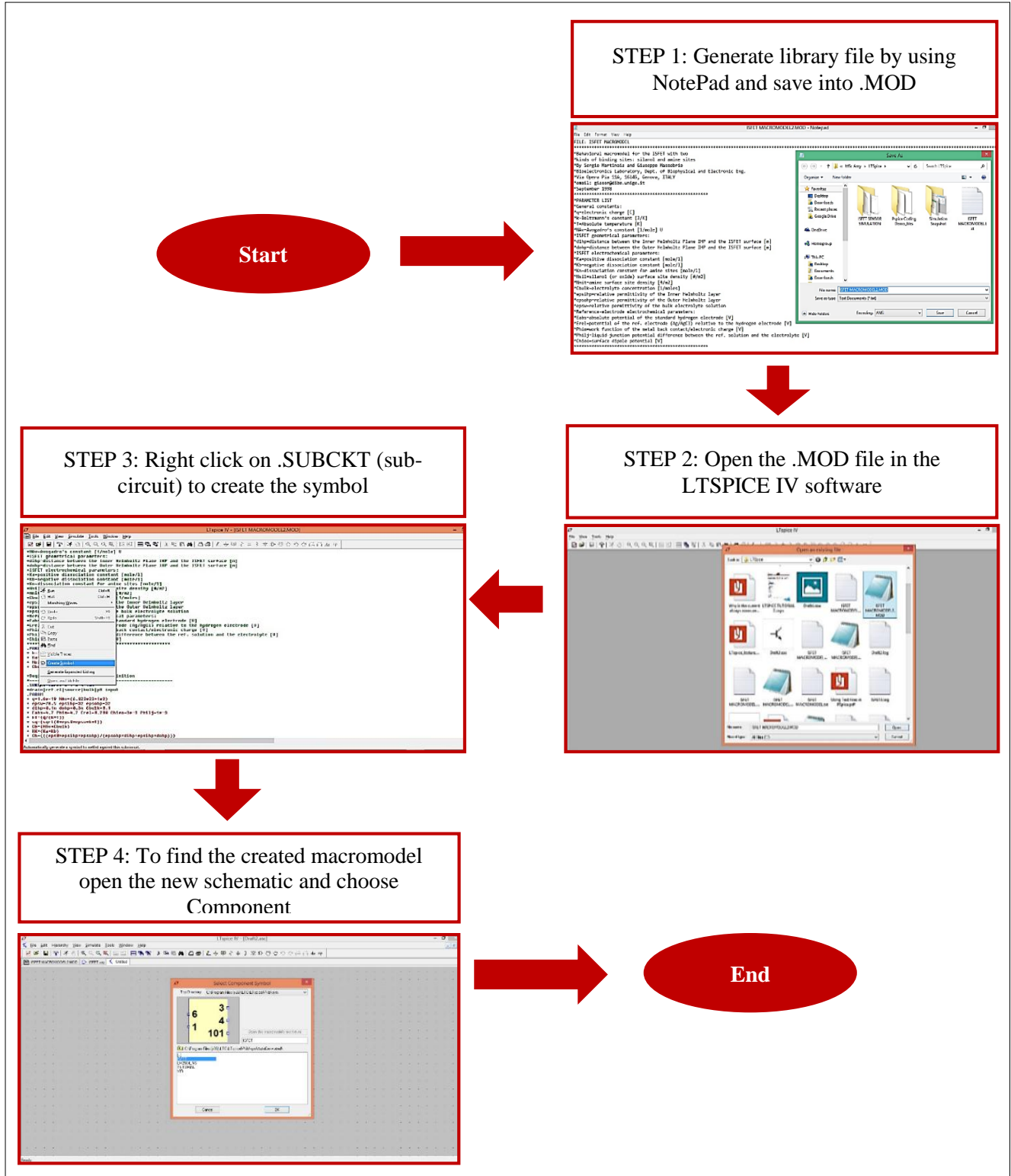


Fig. 5: Steps to integrate and convert the ISFET model into LTSPICE IV software

## 4 Results and Discussion

Result from implementation of ISFET macromodel in LTSPICE IV is shown in Section 4.1. Result from simulation of ISFET macromodel is shown in Section 4.2.

### 4.1 ISFET Macromodel

The ISFET capture symbol that has been created is shown in Fig. 5. Connection point 1 is the Reference electrode Connection point 3 and 6 is the Source and Drain respectively, through which the current flows. Connection point 101 is the output from ISFET.

### 4.2 Simulation of ISFET Macromodel

In order to derive the behavior between  $I_d$  and  $V_{pH}$ , the ISFET macromodel was simulated at optimal  $V_{ref}$ . Fig. 6 displays the variation of  $I_d$  with  $V_d$  at 1.5V of  $V_{ref}$ . It is apparent from this graph that different value of pH resulted different  $I_d$ . The low value of pH 14 and the high value of pH 1 give  $I_d$  at 140 $\mu$ A and 670 $\mu$ A respectively. This shows that low pH yields high  $I_d$ . The graph also shows that  $I_d$  and  $V_d$  is proportional and linear until  $I_d$  is saturated and produce a constant value for each pH value.

$V_{ref}$  of 1.5V has been selected due to the large output current,  $I_d$  compare to the 1.0V of  $V_{ref}$  from pH 1 until pH 14. Table 1 shows the range of output current,  $I_d$ , due to variation in  $V_{ref}$ , at 1.0V and 1.5V. It is apparent from Fig.6 that the ISFET macromodel give a good separation between  $I_d$  for the different pH values.

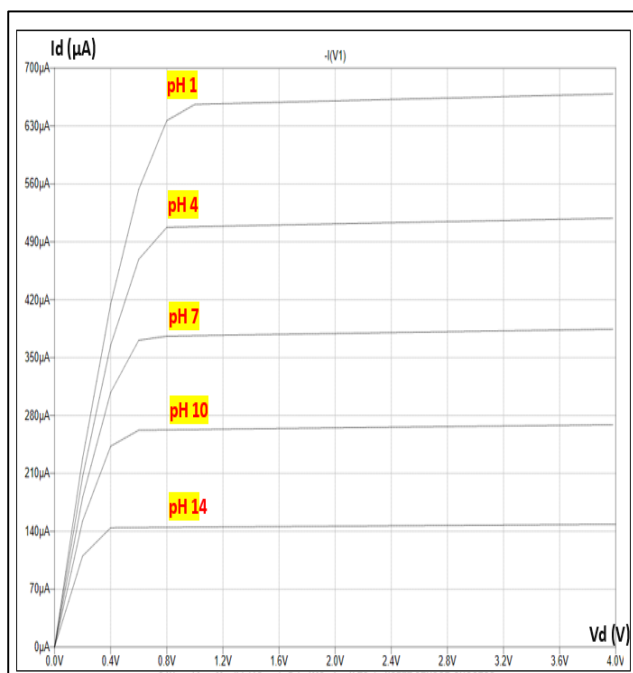


Fig. 6 Graph of  $V_d$  and  $I_d$  vs pH ( $V_{ref} = 1.5V$ )

Table 1 Output current with variation in  $V_{ref}$

$V_{ref}$ (volt)	$I_d$ ( $\mu$ A)
1.0 volt	0-28 $\mu$ A
1.5 volt	0-70 $\mu$ A

## 5 Conclusion

Our work here has illustrated the development of ISFET macromodel in LTSPICE IV from its mathematical model. It is intended to ensure the ISFET macromodel is functioning as its characteristics. From the simulation results, it is decided to use  $V_{ref}$  of 1.5 volts, since the larger output current gives a distinctive separation of drain current between pH 1, pH4, pH7, pH10 and pH 14. It can be conceived that low value of pH or acidic solution draws high value of  $I_d$ , when  $H^+$  ion concentration in the electrolyte solution is high while contrary for high value of pH or alkaline solution.

## Acknowledgment

The author would like to thank the Ministry of Science and Technology (MOSTI) of Malaysia, for providing the research funding, 100-RMI/SF 16/6/2 (14/2015); the Research Management Institute and the Faculty of Electrical Engineering, Universiti Teknologi MARA, Malaysia, for the support and assistance given to the authors in carrying out this research; MIMOS Berhad, Malaysia, for the technical support and permission given to use the facilities in the NAPL laboratory.

## References:

- [1] O. Korostynska, K. Arshak, E. Gill, and a. Arshak, "Review Paper: Materials and Techniques for In Vivo pH Monitoring," *IEEE Sens. J.*, vol. 8, no. 1, pp. 20–28, 2008.
- [2] S. Nomura, "New Challenge to pH Measurement What will come next to the glass electrode?," HORIBA, Ltd. Development Center, Japan, Tech. J., Jul. 13.
- [3] Erich K. Springer, "Improved Process Measurement and Control," Finnesse LLC., Santa Clara, C.A., Tech., 2013.
- [4] Lower, S. K, "Acid-base Equilibria and Calculations," in *General Chemistry Reference Text*, Simon Fraser University, Canada, 1996, pp. 1–48.
- [5] Z. Zulkarnay, S. Shazwani, B. Ibrahim, and A. J. Jurimah, "An Overview on pH Measurement Technique and Application in

- Biomedical and Industrial Process,” *ICoBE*, 2015, pp. 30–31.
- [6] *What is pH and how is it measured?*, Hach Co., Loveland, CO, 2003, pp. 1-23.
- [7] Tom. Hsu, “25.1 Acids, Bases, and pH,” in *Physics and Chemistry, First Edition: Cambridge Physics Outlet*, Peabody, M.A., 2002, pp. 429–435.
- [8] N. I. Georgiev, R. Bryaskova, R. Tzoneva, I. Ugrinova, C. Detrembleur, S. Miloshev, A. M. Asiri, A. H. Qusti, and V. B. Bojinov, “A novel pH sensitive water soluble fluorescent nanomicellar sensor for potential biomedical applications,” *Bioorganic Med. Chem.*, vol. 21, no. 21, pp. 6292–6302, 2013.
- [9] A. V. Legin, E. A. Bychkov, and Y. G. Vlasov, “Analytical applications of chalcogenide glass chemical sensors in environmental monitoring and process control,” *Sensors Actuators B Chem.*, vol. 24, no. 1–3, pp. 309–311, 1995.
- [10] L. A. Schneider, A. Korber, S. Grabbe, and J. Dissemond, “Influence of pH on wound-healing: A new perspective for wound-therapy?,” *Arch. Dermatol. Res.*, vol. 298, no. 9, pp. 413–420, 2007.
- [11] O. Korostynska, K. Arshak, E. Gill, and A. Arshak, “Review on State-of-the-art in Polymer Based pH Sensors,” *Comput. Eng.*, vol. 7, no. 1, pp. 3027–3042, 2007.
- [12] M. Yuqing, C. Jianrong, and F. Keming, “New technology for the detection of pH,” *J. Biochem. Biophys. Methods*, vol. 63, no. 1, pp. 1–9, 2005.
- [13] P. Bergveld, “Thirty years of ISFETOLOGY: What happened in the past 30 years and what may happen in the next 30 years,” *Sensors Actuators, B Chem.*, vol. 88, pp. 1–20, 2003.
- [14] J. Inczedy, T. Lengyel, and A.M. Ure , “8.3.2.4 Ion-selective field effect transistor (ISFET) devices,” in *Compendium of Analytical Nomenclature, Definitive Rules*, Oxford: Blackwell Science, 1998, pp. 6–9.
- [15] G. Massobrio, S. Martinoia, and M. Grattarola, “Ion Sensitive Field Effect Transistor ( Isfet ) Model Implemented in Spice,” *Simulation*, vol. 4, no. 1, 1991.
- [16] S. Martinoia and G. Massobrio, “A behavioral macromodel of the ISFET in SPICE,” *Sensors Actuators B Chem.*, vol. 62, no. 3, pp. 182–189, Mar. 2000.